



Phenology and the response of photosynthesis to irradiance and temperature gradient in the herbal drug red alga, *Chondria armata* (Rhodomelaceae, Ceramiales) from Kagoshima, Japan

Ryuta Terada¹ · Kyosuke Yoshizato² · Kazuma Murakami² · Gregory N. Nishihara³

Received: 11 November 2023 / Revised: 4 April 2024 / Accepted: 8 April 2024
© The Author(s) 2024

Abstract

Seasonal changes in the size of the herbal drug red alga *Chondria armata* (Rhodomelaceae, Ceramiales) were investigated in Kagoshima, Japan, which is near the northern distributional limit in the western Pacific. Additionally, its photosynthetic response to irradiance and temperature was examined using dissolved oxygen sensors and a pulse amplitude modulation (PAM)-chlorophyll fluorometer. This alga was observed in tidepools throughout the year; its height and weight were greatest in December and the lowest in April and May. The net photosynthesis of the photosynthesis–irradiance ($P-E$) curve determined at 28°C quickly saturated at 113 $\mu\text{mol photons m}^{-2} \text{s}^{-1}$, with minimal inhibition even at 1000 $\mu\text{mol photons m}^{-2} \text{s}^{-1}$. The gross photosynthesis of the photosynthesis–temperature ($P-T$) curved over 8 to 40°C, measured at 500 $\mu\text{mol photons m}^{-2} \text{s}^{-1}$, peaked at 30.1°C and decreased rapidly below 20°C and above 36°C, respectively. Similarly, the effective quantum yield ($\Delta F/F_m'$) after a 3-day culture during 4–40°C at 50 $\mu\text{mol photons m}^{-2} \text{s}^{-1}$ remained stable between 16°C and 32°C but decreased outside of this range. The combined effect of irradiance (200 [low] and 1000 [high] $\mu\text{mol photons m}^{-2} \text{s}^{-1}$) and temperature (28, 22, and 16°C) revealed that $\Delta F/F_m'$ declined during exposure to high irradiance at all temperature treatments. However, it mostly recovered after a subsequent 12-hour period of dim-light acclimation at 28°C and 22°C. In contrast, those at 16°C could not recover, indicating the occurrence of low-temperature light stress. This alga appears to be well-adapted to the irradiance and temperature environment at the study site. However, the winter temperature appears to approach its threshold level, and the occurrence of strong light during the winter might adversely affect the abundance of this alga near its northern distributional limit.

Keywords Ecophysiology · Low temperature-light stress · Pulse amplitude modulation (PAM)-chlorophyll fluorometry · Rhodophyta · Seasonal change

Introduction

A red alga, *Chondria armata* (Kützting) Okamura (Rhodomelaceae, Ceramiales), known as '*Hanayanagi*' in Japanese, is widely distributed in the tropical and subtropical

waters of the Pacific and Indian Oceans (Okamura 1907; Silva et al. 1996; Yoshida 1998; Huang 2003; Payri 2006; Huisman 2019). In Japan, this alga is commonly found in the Ryukyu Islands and can also be found in the southern part of the country, particularly along the Pacific Ocean-facing coast in southern Honshu, Shikoku, and Kyushu islands (Okamura 1936; Yoshida 1998). Notably, this alga has been utilized by local inhabitants for many years on the islands of Amami in Kagoshima Prefecture, serving as an herbal drug for anthelmintic purposes, effectively eradicating various intestinal worms such as parasitic roundworms, whipworms, and tapeworms (Tanaka 1956; Shinmura and Tanaka 2008).

From this alga, a natural compound known as domoic acid (DA) has been isolated, and it is believed to be responsible for these therapeutic effects (Takemoto and Daigo 1958; Daigo 1959; Maeno et al. 2018). In fact, the name 'domoic acid' is known to have been derived from the local name for

✉ Ryuta Terada
terada@fish.kagoshima-u.ac.jp

¹ United Graduate School of Agricultural Sciences, Kagoshima University, Kagoshima City, Kagoshima 890-0065, Japan

² Faculty of Fisheries, Kagoshima University, Kagoshima City, Kagoshima 890-0056, Japan

³ Institute for East China Sea Research, Organization for Marine Science and Technology, Graduate School of Integrated Science and Technology, Nagasaki University, Nagasaki City, Nagasaki 851-2213, Japan

this alga, '*Dômoi*,' used on Tokunoshima Island, a remote part of the Amami Islands (Tanaka 1956; Shinmura and Tanaka 2008). However, domoic acid is recognized as the active poison in amnesic shellfish poisoning (ASP), which caused a mass food poisoning incident through the consumption of the mussel *Mytilus edulis* (Mytilidae, Mytilida) that took place in Prince Edward Island, Canada, in 1987 (Wright et al. 1989).

The compound DA in the mussels is reported to be originally produced by the harmful algal bloom-forming diatom genus *Pseudonitzschia* (Bacillariaceae, Bacillariales), leading to its bioaccumulation in shellfish. Therefore, considering that the amount of DA during the ASP outbreaks in mussels in 1987 and other similar incidents were high due to bioaccumulation, it is likely that the levels of the drug derived from *C. armata*, which are ingested for their anthelmintic properties, would be relatively small and have no toxic influence for local inhabitants. Despite phylogenetically far and distinct species groups, these macro and micro algae are reported to have each DA biosynthetic gene cluster with unique origins in their respective hosts (Brunson et al. 2018; Brassart et al. 2022; Steele et al. 2022).

Considering the distinctive attributes of the compound in *C. armata*, it comes as no surprise that numerous studies have been conducted on the constituents of this alga (e.g., Daigo 1959; Maeda et al. 1986, 1987; Zaman et al. 1997; Govenkara and Wahidulla 2000; Ciavatta et al. 2001; Al-Fadhli et al. 2006; Jiang et al. 2014; Mori et al. 2016, 2018; Maeno et al. 2018; Brassart et al. 2022; Steele et al. 2022). However, a significant gap exists in our understanding of the ecology and ecophysiology of this alga. In fact, the phenology of *C. armata*, as well as its adaptations to environmental factors such as irradiance and temperature, remain unexplored and await elucidation.

Our research group has investigated the response of algae to various environmental factors, such as temperature and irradiance gradients using a pulse amplitude modulation (PAM) chlorophyll fluorometry along with dissolved oxygen sensors (Terada et al. 2018, 2021b, c; Borlongan et al. 2019, 2020a, b; Ito et al. 2021, 2023). Furthermore, we have also reported the ecology of several species of both freshwater and marine algae (Nishihara et al. 2004; Shimabukuro et al. 2007a, b; Fujimoto et al. 2014; Terada et al. 2021a; Kurahori et al. 2022). The primary objective of these studies is to gain a deeper comprehension of how algae adapt to their natural habitats, with a specific emphasis on guiding the conservation of macroalgal communities and their diversity.

Remarkably, despite the historical utilization of *C. armata* as an herbal anthelmintic in remote islands in Japan, the ecological and ecophysiological aspects of this alga have remained largely unexplored. In the present study, we conducted a seasonal field survey to elucidate the seasonal variations of this alga in Kagoshima, Japan. Additionally,

we conducted experiments to analyze the photosynthetic response of *C. armata* under varying temperature and irradiance gradients. This endeavor aims to enhance our understanding of the optimal and critical environmental conditions for this alga near the northern distributional limit in the Pacific.

Materials and methods

Phenology

The phenology field survey took place at a large tidepool on the volcanic rocky shore in Hanaze (also known as Hanase; 31.193801 N, 130.508078 E), Ibusuki City, Kagoshima Prefecture, Japan (Supplementary Fig. 1). This study site was the same as the one in our previous study (Steele et al. 2022). The survey dates were as follows: 12 June 2014; 12 July 2014; 26 August 2014; 27 September 2014; 8 November 2014; 10 December 2014; 24 January 2015; 21 February 2015; 18 April 2015; 19 May 2015; and 6 July 2015. During each field survey, ten individuals were randomly collected and then transported to the Laboratory of Marine Botany at Kagoshima University. In the laboratory, measurements were taken for both the height and wet weight of each specimen. The height was defined as the distance from the base of the basal disc to the tip of the branchlet. Wet weight was determined by removing the surface water using Kimwipes (Nippon Paper Creca, Japan). We defined an individual as one that has a single basal disc, even if it has several stems.

To monitor the temperature of the *C. armata* population, a submersible temperature data logger (UA-002-64, Onset Computer, USA) was deployed. This logger recorded the seawater temperature every hour from 13 May 2014 to 12 December 2015, and calculated monthly and daily mean seawater temperatures. Additionally, a submersible quantum data logger (DEFI-L, JFE Advantech, Japan) was placed within the population. It recorded incident irradiance every second from sunrise to sunset on 26 September 2015. The data for incident irradiance was then averaged per minute for subsequent analysis.

Sample collection and stock maintenance for photosynthetic experiments

The samples of *C. armata* used for the photosynthetic experiments were collected from the same study site as the phenology study on 28 August 2014 and 10 and 21 September 2021. The collected algae were promptly transported in a 20 L plastic bottle filled with seawater to the Laboratory of Marine Botany at Kagoshima University. The samples were kept in a 60 L aquarium tank at 24°C, with a salinity of 33 psu, pH of

8.0, and an irradiance of $50 \mu\text{mol photons m}^{-2} \text{s}^{-1}$ (12L:12D photoperiod) until examination. The algae were continuously maintained under these conditions until all laboratory experiments were completed, which took one month.

Oxygenic photosynthesis – irradiance response

Detailed methods for photosynthesis–irradiance (P – E) experiments are explained in our previous studies (e.g. Borlongan et al. 2019, 2020b; Terada et al. 2021c). The samples used in the experiments was collected on 28 August 2014. The net photosynthetic rate was determined at 28°C under irradiance of 0, 30, 60, 100, 150, 200, 250, 500, and $1000 \mu\text{mol photons m}^{-2} \text{s}^{-1}$ ($n = 5$ per irradiance level). The net photosynthetic rate was calculated based on measurements of dissolved oxygen (DO) using DO meters equipped with optical DO sensors (ProODO-BOD, YSI Incorporated, USA). The light source was a metal-halide lamp (MHN-150D-S, Nichido Ind. Co. Ltd, Japan), and irradiance was confirmed using a spherical (4π) submersible quantum sensor (LI-192, LI-250A, LI-COR, USA).

Explant samples (branches and branchlets, approximately 0.2 g wet weight each) were carefully excised and then acclimated overnight in the dark using sterilized natural seawater at 28°C . On the following day, five explants were chosen at random and placed into individual biochemical oxygen demand (BOD) bottles (100 mL, YSI Japan) containing sterilized natural seawater. With utmost care, the DO sensors were inserted into the BOD bottles, ensuring the absence of any trapped air bubbles. DO concentrations were recorded at 5-min intervals over a span of 30 min. This observation period followed a 30-min pre-acclimation under the respective experimental light conditions. Continuous stirring of the seawater was maintained throughout the measurements, and the water temperature was regulated using a water bath equipped with a circuit chiller.

Post-experiment, the exact volumes of the BOD bottles were ascertained and utilized for the computation of photosynthesis and dark respiration rates. To prevent any potential influence from nutrient and dissolved carbon dioxide depletion, the seawater medium was replenished after each exposure and measurement under different light intensities. The P – E experiments commenced at an irradiance of $0 \mu\text{mol photons m}^{-2} \text{s}^{-1}$ and progressed up to $1000 \mu\text{mol photons m}^{-2} \text{s}^{-1}$. Dark respiration and net photosynthetic rates were derived by fitting a first-order linear model to the collected dataset.

Oxygenic photosynthesis – temperature response

Detailed methodologies for conducting photosynthesis–temperature (P – T) experiments were comprehensively outlined in our previous studies (e.g., Ito et al. 2021; Terada et al. 2021c). The samples utilized in these experiments were collected on the same dates as the P – E experiments. The measurements were executed across a spectrum of nine

temperatures (8, 12, 16, 20, 24, 28, 32, 36, and 40°C), with five replicates per temperature ($n = 5$ per temperature level). These experiments were carried out under a constant irradiance of $500 \mu\text{mol photons m}^{-2} \text{s}^{-1}$, determined based on the saturation irradiance at 28°C . The range of temperatures was achieved using a precision water bath. Similar to the approach used in the P – E experiments, explants (approximately 0.2 g wet weight) were sourced from branches and branchlets. Dissolved oxygen (DO) concentrations were measured at 5-min intervals during a 30-min observation period, preceded by a 30-min pre-acclimation to each specific temperature. For the determination of dark respiration rates, a dark acclimation period of 10 min was instituted by enveloping the BOD bottles in aluminum foil.

The temperature response of effective quantum yield ($\Delta F/F_m'$)

Detailed methods for chlorophyll fluorescence measurements using the Mini Imaging-PAM (Heinz Walz GmbH, Germany) have been comprehensively explained in our previous studies (e.g., Terada et al. 2021c, 2023b; Shindo et al. 2022). The experimental samples were obtained on 10 September 2021. One day prior to the experiment, explant samples (branches and branchlets) were cut and allowed to acclimate in the dark at 24°C overnight, ensuring complete acclimation. On the subsequent day, sets of samples ($n = 10$ per temperature level) were placed in 300 mL flasks and cultivated within incubators (Eyela MTI-201B, Tokyo Rikakikai, Japan) at ten different temperatures (4, 8, 12, 16, 20, 24, 28, 32, 34, 35, 36, and 40°C). The cultivation was carried out at $50 \mu\text{mol photons m}^{-2} \text{s}^{-1}$ (12L:12D photoperiod) and continued for a duration of 3 days (with the start of cultivation designated as day 0).

The effective quantum yields ($\Delta F/F_m' = [F_m' - F] / F_m'$) were assessed daily over the 3-day cultivation period at each temperature level. The samples were placed and measured in sterilized natural seawater within a Petri dish (with a diameter of 9 cm) on an aluminum block incubator (BI-536T, Astec, Japan). The temperature during the measurements was regulated using the same aluminum block incubator, and its accuracy was monitored using a thermocouple (testo 925, testo AG, Germany). To establish the initial state, the initial values of $\Delta F/F_m'$ were measured on day 0 prior to initiating the culture experiments; however, these specific data were excluded from the final results.

Effect of continuous irradiance exposures on $\Delta F/F_m'$ at three different temperatures, and their potential of recovery

The $\Delta F/F_m'$ of the samples was tracked using a Mini Imaging-PAM over a 6-h period of exposure to various temperature and irradiance levels, followed by an additional 12-h

acclimation phase under dim light conditions ($20 \mu\text{mol photons m}^{-2} \text{s}^{-1}$; Terada et al. 2021c, 2023b; Shindo et al. 2022). The samples were collected on 21 September 2021. A day prior to the experiment, the samples underwent an overnight pre-incubation in darkness at each temperature treatment (16, 22, and 28°C). Prior to commencing the experiment, initial $\Delta F/F_m'$ values ($n = 10$ per temperature/irradiance treatment) were measured to establish baseline conditions for each treatment combination of irradiance (200 and $1000 \mu\text{mol photons m}^{-2} \text{s}^{-1}$) and temperature (16, 22, and 28°C). Subsequently, the samples were placed in a beaker (300 mL) containing sterile natural seawater, which was maintained at a precise temperature within a water bath (14 L) equipped with a circuit chiller.

During the 6-h duration of exposure to 200 and $1000 \mu\text{mol photons m}^{-2} \text{s}^{-1}$ (utilizing a metal-halide lamp), the samples were continuously agitated using a magnetic stirrer to ensure consistent light exposure across all replicates. The $\Delta F/F_m'$ values ($n = 10$) were assessed every 2 h during the continuous irradiance exposure. Following the 6-h exposure period, the samples were subjected to an acclimation phase under dim light conditions ($20 \mu\text{mol photons m}^{-2} \text{s}^{-1}$) for 12 h, mimicking the duration of the natural night period at their respective experimental temperatures.

After both the 2-h and 12-h periods of dim light acclimation (which corresponds to 8 and 18 h from the initial state), the $\Delta F/F_m'$ measurements were conducted again to validate the potential recovery of PSII.

Modeling the photosynthetic response to temperature and irradiance

The response of photosynthesis to irradiance was examined by modeling the data using an exponential equation (Eq. 1; Jassby and Platt 1976; Webb et al. 1974; Platt et al. 1980; Henley 1993) that included the effects of photoinhibition, which had the form (Borlongan et al. 2019, 2020b):

$$P_{\text{net}} = P_{\text{max}} \left(1 - \exp\left(\frac{-\alpha}{P_{\text{max}}} E\right) \right) \exp\left(\frac{-\beta}{P_{\text{max}}} E\right) - R_d \quad (1)$$

where, P_{net} is the net O_2 production rate, P_{max} is the maximum O_2 production rate, α is the initial slope of the P - E curve, β which is a parameter to model the effects of photoinhibition, E is the incident irradiance, and R_d is the dark respiration rate. From this model, the saturation irradiance (E_k) was calculated as P_{max} / α and the compensation irradiance (E_c) was $P_{\text{max}} \ln\left(\frac{P_{\text{max}}}{P_{\text{max}} - R_d}\right) / \alpha$ when β is zero.

The model was fitted using Bayesian methods, where the parameters were given a Gaussian prior with a location of 0 and a scale of 1. The model parameters were fitted on the log-scale to ensure positive values. A scaled Student's

t-distribution with 3 degrees-of-freedom, a location of 0, and a scale of 2 was the prior for the error term, which was assumed to be Gaussian distributed.

A generalized additive model was used to analyze the oxygenic photosynthesis and temperature experiment (Eq. 2).

$$\Delta F/F_m' = a_{0,\text{day}} + s(\text{temperature}, \text{day}) + s(\text{temperature}) \quad (2)$$

where, $\Delta F/F_m'$ is the effective quantum yield measured during the experiment, $a_{0,\text{day}}$ is the model intercept, $s(\text{temperature}, \text{day})$ is a smooth function of temperature and day, and $s(\text{temperature})$ is a smooth function of temperature. In this formulation, the $s(\text{temperature}, \text{day})$ smooth function represents the effect of day on the general smooth function of temperature. The basis for the smooth function was a Duchon spline (5 basis functions), and the distribution was assumed to follow a zero-inflated Beta distribution (Ospina and Ferrari 2012). The zero-inflation rate was also assumed to follow a similar model with two smooths and an intercept, and the precision parameter for the Beta distribution was allowed to vary with day. The model was fit with a logit link function for the observations and the zero-inflation rate, whereas the precision parameter was fit using a log link function. This model was also fitted using Bayesian methods, where Student's t-distribution with 3 degrees of freedom, a location of 0, and a scale of 2 was used for the prior distribution for all model parameters.

The effect of temperature on the photosynthetic rate was analyzed using a thermodynamic model (Alexandrov and Yamagata 2007). Here, the gross photosynthetic rate (GP), is treated as a latent variable, which is assumed to be equal to the sum of the net photosynthetic rate (NP) and the dark respiration (R_d). Under light, photorespiration and non-photorespiratory reactions consume oxygen (Tcherkez et al. 2008). Often respiration rates under darkness and light are assumed to be negligible (Bellasio et al. 2014), hence in this model we assume that respiration under light can be approximated by the dark respiration rates.

$$NP = \frac{y_{\text{max}} H_a \exp\left(\frac{H_a(x-x_{\text{opt}})}{xR_{x_{\text{opt}}}}\right)}{\left(H_d - H_a \left(1 - \exp\left(\frac{H_d(x-x_{\text{opt}})}{xR_{x_{\text{opt}}}}\right)\right)\right)} - R_d \quad (3)$$

$$R_d = R_{20} \exp\left(-\frac{E_a}{R} (x^{-1} - x_{20}^{-1})\right)$$

There are five parameters in the model, where x_{opt} is the absolute temperature that maximizes the NP , y_{max} is the NP at x_{opt} , and H_a and E_a are represents the activation energy. H_d is the deactivation energy. The constant R is the ideal gas constant with a value of $8.314 \text{ J mol}^{-1} \text{ K}^{-1}$, R_{20} is the respiration rate at an arbitrary reference temperature (i.e., 20°C).

This model was analyzed using Bayesian methods. The net photosynthesis rate was assumed to follow a normal

distribution, whereas the dark respiration was modeled assuming a Gamma distribution and a log link function. A normal distribution was used for the parameters and a Student's *t*-distribution (3 degrees of freedom, location of 0, and a scale of 2) was used for the scale of the normal and Gamma distribution. Details of the prior distribution for the model parameters are provided in the supplement (Supplementary table S1).

Statistical analyses

Statistical analyses for all models were executed using *R* version 4.3.0 (R Development Core Team 2023). The process of model fitting was conducted utilizing the *brms* package version 2.19.0 (Bürkner 2018), with parameter estimation achieved through Bayesian methodologies. The *brms* package, integrated with *RStan* (Stan Development Team 2024), was employed as the computational backend to draw samples from the posterior distributions of the parameters.

Besides the Bayesian analysis of the models, we were also interested in testing the null hypothesis that there were no pair-wise differences in the means of 4 exposure times (i.e., 0, 6, 8, and 18) with each irradiance and temperature treatment of the continuous irradiance exposure experiment. A Tukey's HSD test was used in the analysis, with a significance level of 0.05.

Results

Phenology

At the study site this alga was found in the tidepool at the depth of 0.5 – 1 m deep during low tide and was never exposed in air even at the spring low tide. During the study period the height of *C. armata* exhibited a gradual increase starting from June 2014, measuring at 2.40 ± 0.56 cm (mean \pm standard deviation, SD; Fig. 1a). The highest height was recorded in December 2014, reaching 4.65 ± 0.75 cm. Subsequently, a gradual decrease was observed, reaching its lowest point in April 2015, at 1.91 ± 0.67 cm. Terminal branchlets had been gradually decaying or disappearing from the algal body since December. However, the basal disc and stems (main axis) remained intact, while branchlets had gradually reemerged and increased since along with newly recruited individuals (Fig. 2). Following this, another period of gradual increase occurred, with the height reaching 2.68 ± 0.47 cm in July. A similar trend was noticed in the wet weight of the algae (Fig. 1b). Commencing in April 2014, the wet weight of the algae exhibited a gradual increase, measuring 1.73 ± 1.08 g. The highest weight was recorded in December, reaching 5.94 ± 2.15 g. This was followed by a gradual decrease in the wet weight, with the lowest value

observed in May 2015, at 0.94 ± 0.39 g. Once again, a slight increase was noted in July, with the weight measuring at 1.48 ± 0.55 g. Tetrasporangia were confirmed on the terminal portion of the branchlets at times between August and December with regard to the reproductive cells; however, no spermatangia or cystocarp could be found.

Throughout the study period the seawater temperature within the *C. armata* population displayed distinct seasonal fluctuations (Fig. 3). The recording commenced in May 2014, revealing a monthly average temperature of $21.6 \pm 0.92^\circ\text{C}$. The highest monthly mean seawater temperature in 2014 occurred in August, peaking at $27.6 \pm 0.98^\circ\text{C}$. Subsequently there was a gradual decline in seawater temperature, reaching its lowest point in February 2015, with an average of $16.1 \pm 0.83^\circ\text{C}$. Following this cooling trend there ensued another phase of gradual temperature increase. By August 2015 the monthly mean seawater temperature had risen to $28.5 \pm 0.67^\circ\text{C}$. However, as the recording period ended in December, the seawater temperature exhibited a decrease

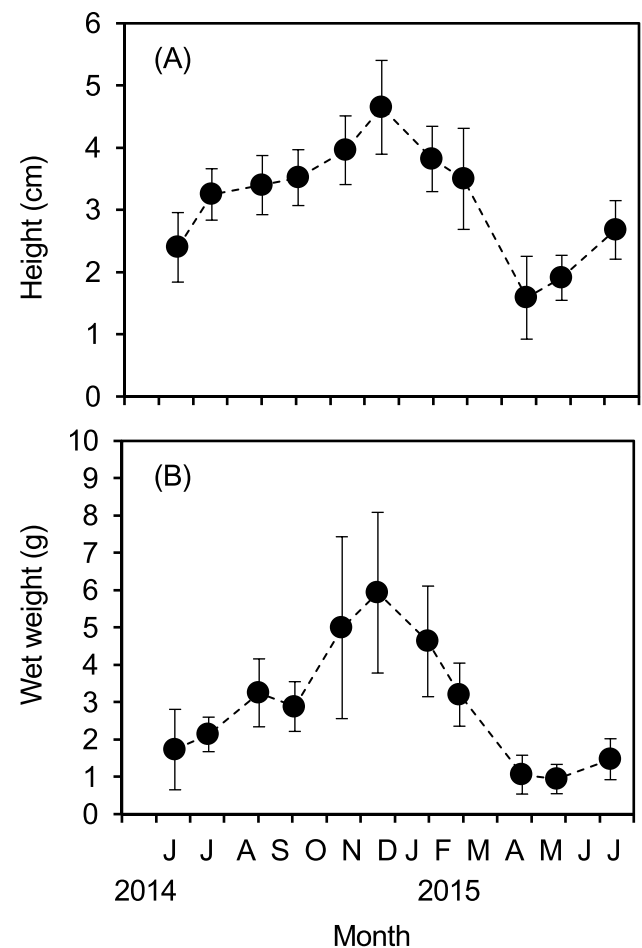
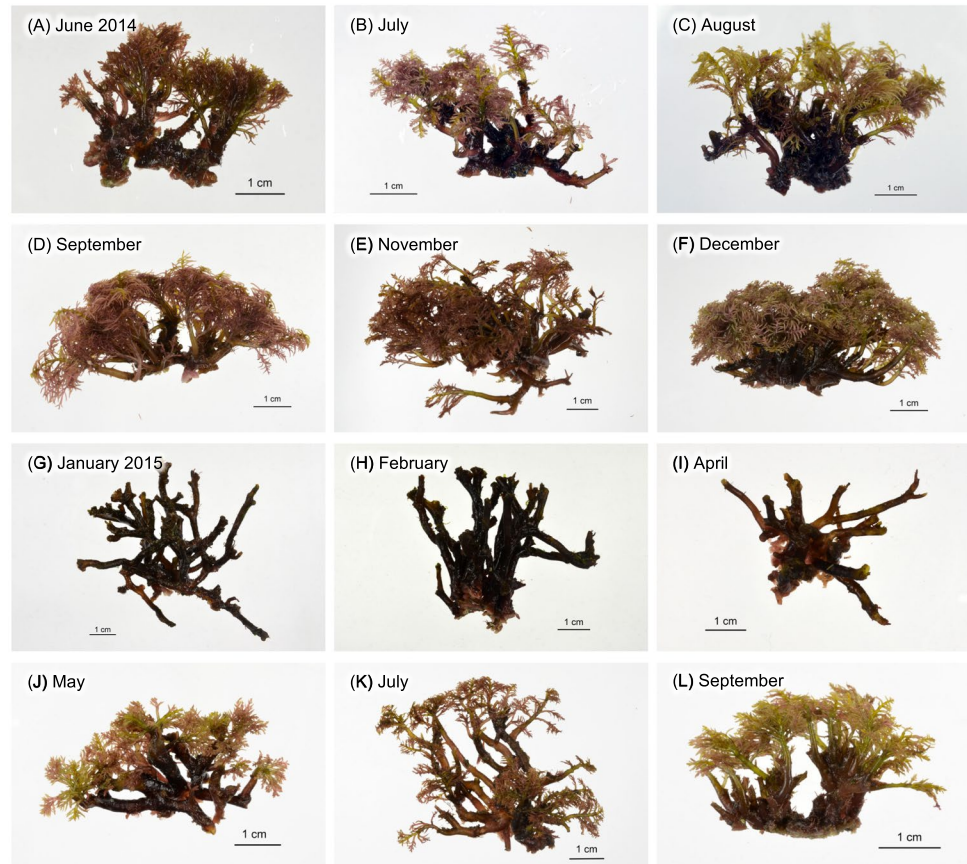


Fig. 1 Seasonal changes in height (A) and wet weight (B) of a red alga, *Chondria armata* from Kagoshima, Japan, during June 2014 to July 2015. Symbols and bars represent the mean and standard deviation of observations ($n = 10$)

Fig. 2 Photos showing the various habits of a red alga (A–L), *Chondria armata*, taken in Kagoshima, Japan, from June 2014 to September 2015. (A) June 2014, (B) July 2014, (C) August 2014, (D) September 2014, (E) November 2014, (F) December 2014, (G) January 2015, (H) February 2015, (I) April 2015, (J) May 2015, (K) July 2015, (L) September 2015



once more, settling at $22.3 \pm 0.68^\circ\text{C}$. The highest and lowest daily mean seawater temperature were $29.6 \pm 0.61^\circ\text{C}$ (10 August 2015) and $14.5 \pm 1.32^\circ\text{C}$ (15 February 2015), respectively.

On 26 September 2014 underwater irradiance displayed dynamic fluctuations starting from sunrise at 6 AM and continuing until sunset at 6 PM (Fig. 4). The peak mean irradiance per minute ($1288 \pm 44.7 \mu\text{mol photons m}^{-2} \text{s}^{-1}$) occurred at noon time (12:40). Throughout that day the weather remained fine with a clear sky until sunset. However, the sunlight on the habitat was shaded by rocky walls from sunrise until just before noon (Fig. 4). *Chondria armata* remained submerged in seawater throughout the measurement period, and there were no other algae that covered this species (Supplementary Fig. 1).

Oxygenic photosynthesis – irradiance response

As the irradiance was elevated to $1000 \mu\text{mol photons m}^{-2} \text{s}^{-1}$ the measured net photosynthetic (NP) rate displayed a linear increase that subsequently reached saturation, with values of $14.23 \pm 2.56 \mu\text{g O}_2 \text{g}_{\text{ww}}^{-1} \text{min}^{-1}$ at $500 \mu\text{mol photons m}^{-2} \text{s}^{-1}$ and $12.08 \pm 2.19 \mu\text{g O}_2 \text{g}_{\text{ww}}^{-1} \text{min}^{-1}$ at $1000 \mu\text{mol photons m}^{-2} \text{s}^{-1}$ (Fig. 5). Utilizing the model-fitted $P-E$

curve, we estimated the maximum NP rate (NP_{max}) to be 24.7 (HDCI: $21.7 - 28.0$) $\mu\text{g O}_2 \text{g}_{\text{ww}}^{-1} \text{min}^{-1}$ (Table 1). Furthermore, the compensation (E_c) and saturation irradiances

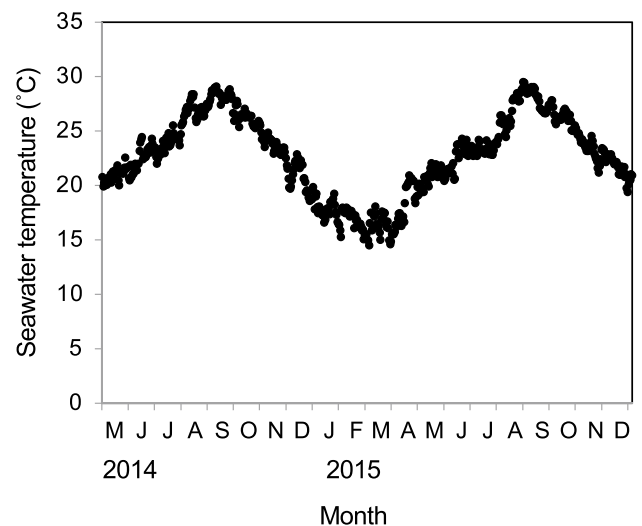


Fig. 3 Seasonal changes in daily mean seawater temperature for the population of a red alga, *Chondria armata* from Kagoshima, Japan, during May 2014 through December 2015. Symbols indicate daily mean seawater temperatures measured every hour

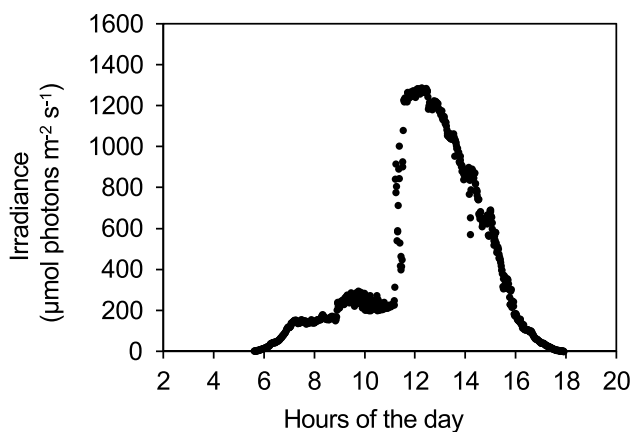


Fig. 4 Diurnal changes in *in situ* irradiance for the population of a red alga, *Chondria armata* from Kagoshima, Japan, on 26 September 2014. Measurements were taken every second, and symbols represent the mean values for each minute

(E_k) were estimated to be 8.7 (HDCI: 6.8 – 10.6) and 113.2 (HDCI: 86.5 – 143.7) $\mu\text{mol photons m}^{-2} \text{s}^{-1}$, respectively (Table 1). Detailed parameter estimates can be found in Table 1.

Oxygenic photosynthesis – temperature response

The temperature response of both net and gross photosynthesis, spanning from 8 to 40°C at 500 $\mu\text{mol photons m}^{-2} \text{s}^{-1}$, exhibited a temperature-dependent decline with a single peak (Fig. 6). The measured net NP rate exhibited an increment from $-0.87 \pm 0.42 \mu\text{g O}_2 \text{g}_{\text{ww}}^{-1} \text{min}^{-1}$ at 8°C, peaking at a maximum of $11.37 \pm 1.91 \mu\text{g O}_2 \text{g}_{\text{ww}}^{-1} \text{min}^{-1}$ at 28°C, and subsequently decreasing to $-14.12 \pm 1.70 \mu\text{g O}_2 \text{g}_{\text{ww}}^{-1} \text{min}^{-1}$ at 40°C. Measured dark respiration rates displayed an increase as the temperature rose, reaching a maximum of $18.75 \pm 3.55 \mu\text{g O}_2 \text{g}_{\text{ww}}^{-1} \text{min}^{-1}$ at 40°C.

By employing the model-fitted gross photosynthesis–temperature (P – T) response derived from NP and dark respiration rates, optimal temperature ($T_{\text{opt}}^{\text{GP}}$) was estimated to be 30.1°C (HDI: 28.9 – 31.4) at the maximum gross photosynthetic rate ($GP_{\text{max}} = 20.2 \mu\text{g O}_2 \text{g}_{\text{ww}}^{-1} \text{min}^{-1}$, HDCI: 18.6 – 21.7). According to the model, the dark respiration rate at 20°C (R_{20}) was estimated to be $1.3 \mu\text{g O}_2 \text{g}_{\text{ww}}^{-1} \text{min}^{-1}$ (HDCI: 1.2 – 1.4). Detailed parameter estimates can be found in Table 2.

The temperature response of effective quantum yield ($\Delta F/F_m'$)

The temperature response of effective quantum yield of photosystem II ($\Delta F/F_m'$), spanning from 4 to 40°C in 3-day culture under a 50 $\mu\text{mol photons m}^{-2} \text{s}^{-1}$ (12:12D photoperiod), demonstrated a temperature-dependent decline with a single

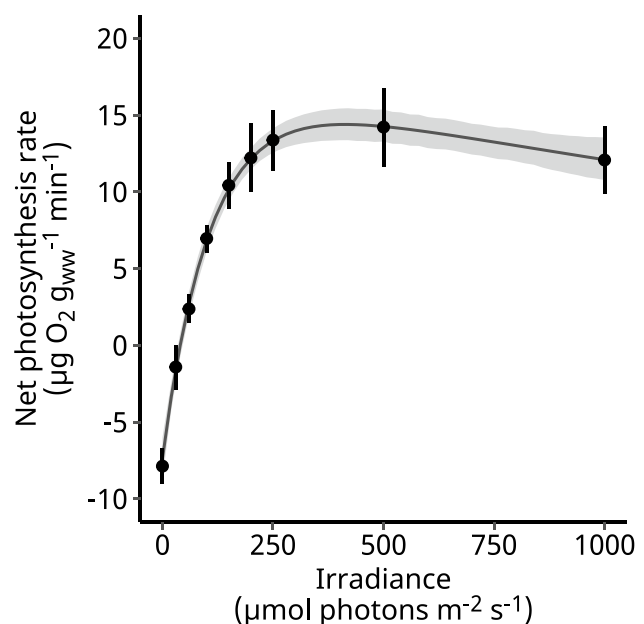


Fig. 5 Response of net photosynthetic rates in a red alga, *Chondria armata* from Kagoshima, Japan, to irradiance (0–1000 $\mu\text{mol photons m}^{-2} \text{s}^{-1}$) at 28°C. Symbols and bars represent the mean and standard deviation of observations ($n = 5$ per irradiance), while lines depict the expected photosynthesis–irradiance model curve. The shaded region indicates the 95% credible intervals of the model

peak (Fig. 7a, b, c). Throughout the 3-day culture, measured $\Delta F/F_m'$ values remained relatively stable at 20, 24, and 28°C (0.524 ± 0.015 , 0.529 ± 0.010 , 0.523 ± 0.014 for the 3-day duration). However, values beyond this range gradually diminished or even reached zero during the 3-day culture period. Notably, $\Delta F/F_m'$ values below 12°C and above 36°C nearly approached or entirely reached zero. The expected values estimated from the model of the $\Delta F/F_m'$ – temperature response can be found in Supplementary table S2.

Table 1 The mean and 95% highest density credible intervals (95% HDCI) of photosynthesis–irradiance (P – E) parameters of a red alga, *Chondria armata* from Kagoshima, Japan at 28°C. NP_{max} = maximum net photosynthesis ($\mu\text{g O}_2 \text{g}_{\text{ww}}^{-1} \text{min}^{-1}$); α = initial slope [$\mu\text{g O}_2 \text{g}_{\text{ww}}^{-1} \text{min}^{-1} (\mu\text{mol photons m}^{-2} \text{s}^{-1})^{-1}$]; R_d = respiration rate ($\mu\text{g O}_2 \text{g}_{\text{ww}}^{-1} \text{min}^{-1}$); E_c = compensation irradiance ($\mu\text{mol photons m}^{-2} \text{s}^{-1}$); E_k = saturation irradiance ($\mu\text{mol photons m}^{-2} \text{s}^{-1}$); β = parameter to model the effects of photoinhibition

Parameter	Mean	95% HDCI
NP_{max}	24.7	21.7 – 28.0
α	0.221	0.180 – 0.262
R_d	7.3	6.0 – 8.7
E_c	8.7	6.8 – 10.6
E_k	113.2	86.5 – 143.7
β	0006	0.001 – 0.011

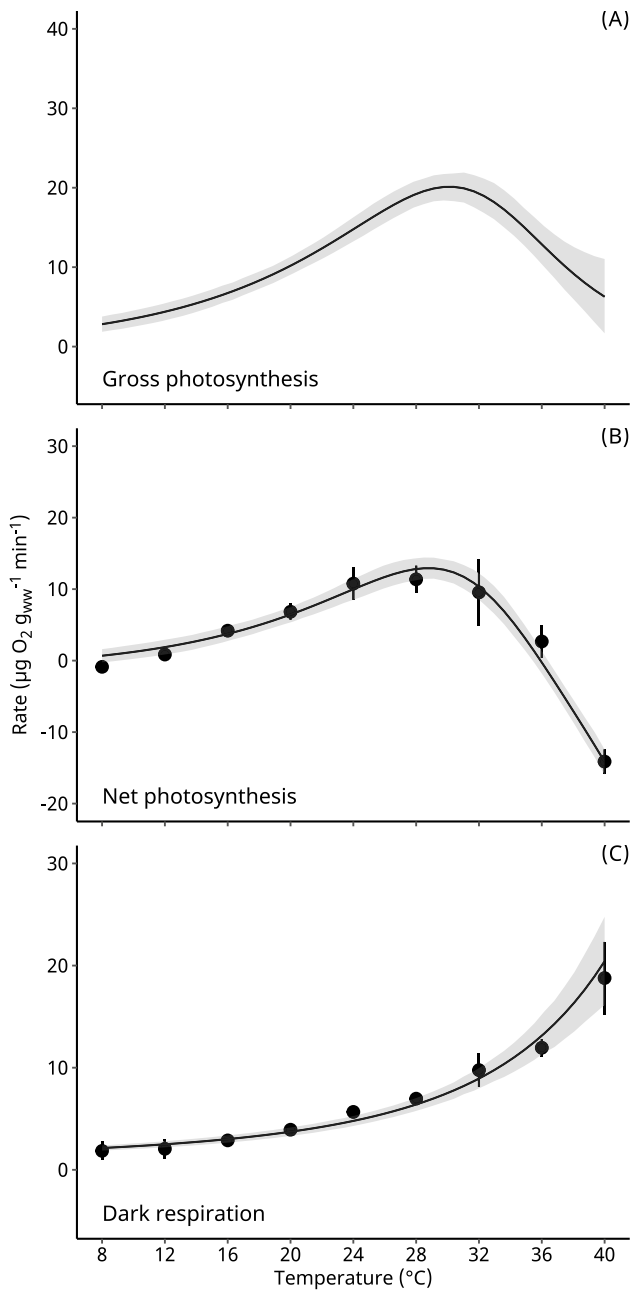


Fig. 6 Response of oxygenic gross photosynthesis (A), net photosynthesis (B), and dark respiration rates (C) in a red alga, *Chondria armata* from Kagoshima, Japan, to temperature (8, 12, 16, 20, 24, 28, 32, 36, and 40°C). Net photosynthesis measurements were conducted at 500 $\mu\text{mol photons m}^{-2} \text{s}^{-1}$, and dark respiration at 0 $\mu\text{mol photons m}^{-2} \text{s}^{-1}$. Gross photosynthesis data were derived from the model curves of net photosynthesis (B) and dark respiration (C). Symbols and bars represent the mean and standard deviation of observations ($n = 5$). The shaded region indicates the 95% credible intervals of the model

Table 2 The mean and 95% highest density credible intervals (95% HD CI) of the parameters estimated for the gross photosynthesis – temperature model of a red alga, *Chondria armata* from Kagoshima, Japan at 500 $\mu\text{mol photons m}^{-2} \text{s}^{-1}$. GP_{max} = maximum gross photosynthesis ($\mu\text{g O}_2 \text{ g}_{\text{ww}}^{-1} \text{ min}^{-1}$); H_a = activation energy for photosynthesis (kJ mol^{-1}); H_d = deactivation energy (kJ mol^{-1}); T_{opt}^{GP} = optimum temperature ($^{\circ}\text{C}$); E_a = activation energy for respiration (kJ mol^{-1}); R_{20} = respiration rate at 20°C ($\mu\text{g O}_2 \text{ g}_{\text{ww}}^{-1} \text{ min}^{-1}$). Note that 1 eV = 96.485 kJ mol^{-1}

Parameter	Mean	95% HD CI
GP_{max}	20.2	28.9 – 31.4
H_a	75	58 – 94
H_d	265	208 – 327
T_{opt}^{GP}	30.1	28.9 – 31.4
E_a	32	27 – 36
R_{20}	1.3	1.3 – 1.4

Effect of continuous irradiance exposures on $\Delta F/F_m'$ at three different temperatures, and their potential of recovery

Various characteristic responses in $\Delta F/F_m'$ were observed under different 6-hour exposure combinations involving irradiance and temperature, as well as the potential for recovery during subsequent 12-h dim-light acclimation (Fig. 8).

At 16°C, when algae were exposed to the irradiance of 200 $\mu\text{mol photons m}^{-2} \text{s}^{-1}$, the $\Delta F/F_m'$ appeared to moderately decline after 6 h of exposure, with the $\Delta F/F_m'$ after 6 h (0.347 ± 0.018) at 79.4% ($P < 0.0001$) of the initial $\Delta F/F_m'$ (0.436 ± 0.012 ; Fig. 8A). Following a subsequent 12-h dim-light acclimation, their final $\Delta F/F_m'$ (0.447 ± 0.022) fully recovered, exceeding the initial value by 2.4% ($P = 0.7650$). On the other hand, those exposed to high irradiance exhibited a significant drop to 0.056 ± 0.003 after 6 h, reaching 14.3% ($P < 0.0001$) of the initial $\Delta F/F_m'$ (0.393 ± 0.033 ; Fig. 8B). After a 12-h dim-light acclimation, their $\Delta F/F_m'$ (0.095 ± 0.047) remained notably lower than the initial $\Delta F/F_m'$ by 24.2% ($P < 0.0001$).

At 22°C, algae exposed to low irradiance similarly maintained their $\Delta F/F_m'$ during the 6-h exposure, with the $\Delta F/F_m'$ after 6 h (0.400 ± 0.026) at 89.4% ($P = 0.0008$) of the initial $\Delta F/F_m'$ (0.447 ± 0.026 ; Fig. 8C). Following a subsequent 12-h dim-light acclimation, their final $\Delta F/F_m'$ (0.455 ± 0.022) fully recovered to 101.8% ($P = 0.8914$) of the initial $\Delta F/F_m'$. Conversely, for algae exposed to high irradiance, their 6-h $\Delta F/F_m'$ (0.120 ± 0.012) represented a 25.8% ($P < 0.0001$) drop from the initial $\Delta F/F_m'$ ($0.465 \pm$

0.030; Fig. 8D). After 12 h of dim-light acclimation, their final $\Delta F/F_m'$ (0.401 ± 0.033) almost fully recovered to 86.3% ($P = 0.0008$) of the initial $\Delta F/F_m'$.

At 28°C, algae exposed to low irradiance also maintained their $\Delta F/F_m'$ during the 6-h exposure, with the $\Delta F/F_m'$ after 6 h (0.434 ± 0.012) at 97.7% ($P = 0.4644$) of the initial $\Delta F/F_m'$ (0.444 ± 0.016 ; Fig. 8E). Following a subsequent 12-h dim-light acclimation, the $\Delta F/F_m'$ fully recovered to 0.479 ± 0.018 , exceeding the initial value by 7.8% ($P < 0.0001$). Conversely, algae exposed to high irradiance exhibited a typical decline in $\Delta F/F_m'$, dropping from an initial value of 0.426 ± 0.021 to 0.157 ± 0.016 after 6 h at 36.9% ($P < 0.0001$) of the initial $\Delta F/F_m'$ (Fig. 8F). Following a 12-h dim-light acclimation, their final $\Delta F/F_m'$ increased to 0.404 ± 0.044 , reaching 94.7% ($P < 0.0001$) of the initial $\Delta F/F_m'$.

Discussion

In Japan this alga is primarily distributed in the subtropical Ryukyu Islands (Tanaka 1956; Yoshida 1998; Shinmura and Tanaka 2008). Nevertheless, its distribution extends beyond the Ryukyu Islands, encompassing temperate more northern regions of the country, especially along the Pacific Ocean-facing coasts of southern Honshu (Wakayama Prefecture; 33° N), Shikoku (Kochi Prefecture; 33° N), and Kyushu islands (Kagoshima Prefecture; 31° N; Source: Specimens at SAP, Hokkaido University Museum). The study site we had chosen (Steele et al. 2002), situated in the southern part of Kyushu Island, does not mark the definitive northern distributional limit for this alga. However, since these areas within its distribution in mainland Japan are consistently influenced by the warm Kuroshio Current (Japan Current), there is a near uniformity in the annual range of seawater temperature (16–28°C) across these regions (Serisawa et al. 1998; Nishihara et al. 2004; Shimabukuro et al. 2007b). In this sense, the annual range of seawater temperature, including the lowest temperature at our study site, closely resembles that of the alga's northern distributional limit (16°C).

In the present study this alga could be found on the substrata throughout a year with the characteristic seasonal changes. Indeed, terminal branchlets had been steadily decaying or disappearing from the algal body since December, when the seawater temperature dropped below 20°C. However, the basal disc and main branches remained intact during the winter, while branchlets gradually reemerged and proliferated starting from April, when the seawater temperature increased above 20°C. In addition to these old individuals, newly recruited individuals also appeared and grew alongside them. Consequently, the algae demonstrated gradual growth throughout the summer and extending into late autumn. A year-round occurrence of this alga was also reported from the Taiwan entity (Wang and Chiang 1994).

In the temperate region of Japan, which includes Kyushu Island, temperate species of marine algae typically exhibit distinct seasonality, prevailing from spring to early summer (April–June) and diminishing by midsummer in August (e.g., Shimabukuro et al. 2007a, b; Kurahori et al. 2022). Contrastingly, even within the same region, the seasonality of tropical/subtropical algae exhibits some variation, flourishing consistently from summer through early winter. In this context, the seasonality pattern observed in *C. armata* during the present study resembled that of the tropical red alga, *Laurencia brongniartii* J. Agardh (Rhodomelaceae, Ceramiales), which was documented near the study site (Nishihara et al. 2004).

In the present study confirmation of any sexual reproduction was not possible. Indeed, the species of *Chondria*, including this alga, is known to have an isomorphic life cycle that alternates between gametophyte and sporophyte stages, exhibiting the same macroscopic appearances (*Poly-siphonia*-type; Tani and Masuda 2003). However, in certain species of the genus *Chondria*, the presence of reproductive gametophytes has either not been confirmed or is exceedingly rare. Indeed, a red alga, *Chondria crassicaulis* Harvey (Rhodomelaceae, Ceramiales) is prevalent in its reproductive sporophyte form, while its gametophyte form is considered to be infrequent, occasionally found on the brown alga *Sargassum fusiforme* (Harvey) Setchell (Sargassaceae, Fucales) as an attached organism (Yamagishi and Miwa 2008). Since it remains uncertain whether the gametophyte of *C. armata* inhabits a distinct environment or coexists with the sporophyte, additional research is imperative to gain a more comprehensive understanding of this alga's ecological dynamics in connection with its life cycle.

The range of seawater temperature during the period of abundance for this alga was closely linked to its optimal temperatures, as indicated by the temperature responses in oxygenic photosynthesis and $\Delta F/F_m'$. Indeed, considering that both oxygenic gross photosynthesis and $\Delta F/F_m'$ exhibited rapid declines at temperatures below 20°C and 16°C, respectively, it becomes evident that low temperatures exert an inhibitory effect on the photosynthetic activities of this alga. Therefore, the winter temperature at the study site appears to be tolerable but in close proximity to the threshold level for efficient photosynthesis and survival. It is worth noting that this alga is absent in more northern regions where winter monthly seawater temperatures drop below 15°C; thus, a temperature above 16°C could be deemed critical for the survival of this alga. In fact, it is recognized that low temperatures inhibit the fixation of carbon dioxide, resulting in the generation of reactive oxygen species (ROS). These ROS, in turn, suppress the *de novo* synthesis of the D₁ protein, exacerbating the impairment of PSII repair and ultimately leading to more pronounced damage to PSII (Allakhverdiev and Murata 2004).

In contrast, due to its widespread distribution in the tropical waters of the Pacific and Indian Oceans, this alga exhibited a relatively robust tolerance to high temperatures exceeding 28°C, as observed in oxygenic gross photosynthesis and $\Delta F/F_m'$. This adaptability could potentially account for its consistent presence during the summertime. However, considering the decrease in $\Delta F/F_m'$ and oxygenic gross photosynthesis beyond 36°C, it is plausible that heat stress is taking place, consequently leading to PSII deactivation. This could be attributed to thermal stress causing structural rearrangements in the thylakoid membranes (Roleda 2009) or to an accumulation of hydrogen peroxide, which impedes the de novo synthesis of the D₁ protein in PSII (Allakhverdiev and Murata 2004; Allakhverdiev et al. 2008; Takahashi and Murata 2008). However, based on the recorded seawater temperatures within the tidepool, it is evident that the monthly and daily mean temperatures did not surpass 30°C. This suggests that this alga is well adapted to the temperature conditions present at the study site.

The diurnal variation in incident irradiance revealed the highest minute-averaged irradiance around noon under clear skies, reaching 1200 $\mu\text{mol photons m}^{-2} \text{s}^{-1}$. However, exposure to this relatively strong irradiance seemed to be limited only to the midday period when the sky was clear. In fact, the response of net photosynthesis in the *P-E* curve at 28°C indicated a low light adaptation, with compensation and saturation irradiances showing relatively low values.

Results from combined irradiance and temperature experiments also indicated that there was little influence during exposure to low irradiance (200 $\mu\text{mol photons m}^{-2} \text{s}^{-1}$) at three temperatures, with full recovery of $\Delta F/F_m'$ observed after subsequent 12-h acclimation to dim light. However, under high irradiance exposure, a strong influence on $\Delta F/F_m'$ was observed after 6 h of exposure, suggesting the occurrence of photoinhibition. Nevertheless, $\Delta F/F_m'$ at 28°C and 22°C treatments almost fully recovered after subsequent acclimation, signifying the potential for recovery from this inhibitory stress. More interestingly, those exposed to high irradiance at 16°C showed a greater enhancement in the reduction of $\Delta F/F_m'$ during exposure and did not return to the initial levels even after acclimation to dim light, suggesting the occurrence of low temperature-induced photoinhibition.

In our previous studies, similar sensitivities were also observed in various tropical and temperate species, including *Caulerpa lentillifera* J. Agardh (Caulerpaceae, Bryopsidales), *Ryugophycus kuaweuweu* (Spalding and Sherwood) Kawai et al. (Ulvaceae, Ulvales), as well as *Sargassum patens* C. Agardh and *Sargassum macrocarpum* C. Agardh (Sargassaceae, Fucales; Terada et al. 2018, 2020, 2021c, 2023b). Therefore, the presence of intense irradiance during winter temperatures might serve as one of the limiting factors influencing the flourishing or decline of each species at the northern distribution limits. Possibly, the absence of *C. armata* in the northern regions of

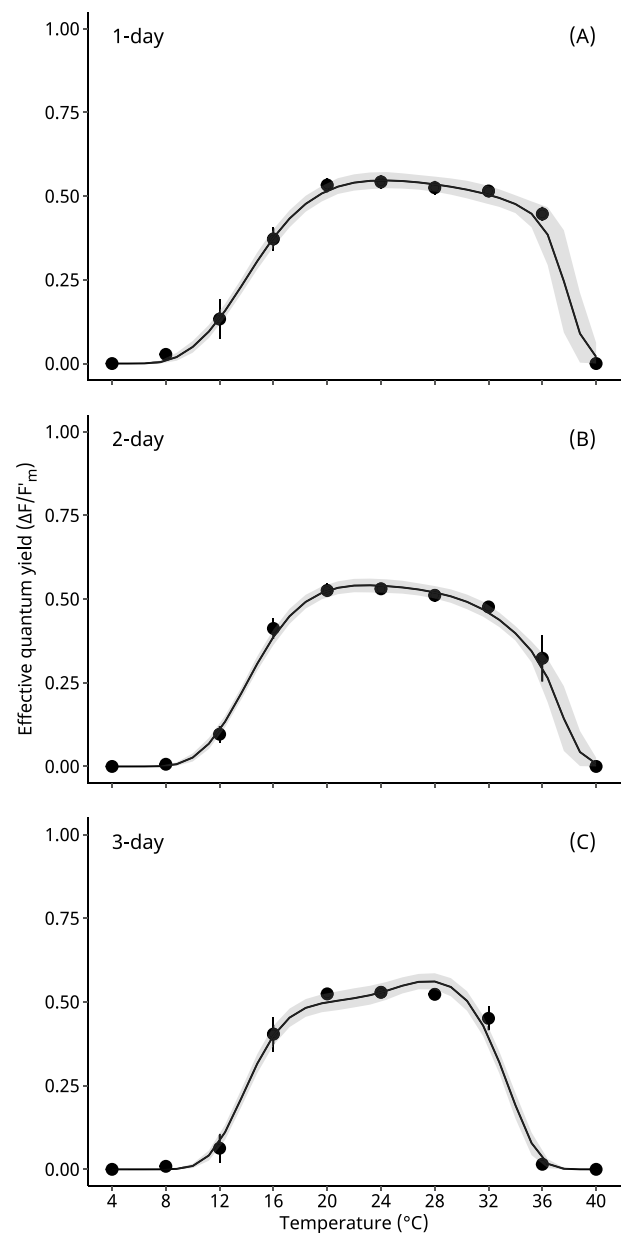


Fig. 7 Response of effective quantum yields of photosystem II ($\Delta F/F_m'$) in a red alga, *Chondria armata* from Kagoshima, Japan, to ten temperature treatments (4, 8, 12, 16, 20, 24, 28, 32, 36, and 40°C) after 1- (A), 2- (B), and 3-day (C) culture under 50 $\mu\text{mol photons m}^{-2} \text{s}^{-1}$ (12L:12D photoperiod). Symbols and bars represent the mean and standard deviation of observations ($n = 10$). The line indicates the generalized additive model (GAM), and the shaded region indicates the 95% credible interval

Japan proper might be influenced not only by temperature but also by the intensity of incident light during winter.

This alga appears to be well adapted to relatively strong irradiance in our photosynthetic experiment, and this insight seems appropriate as this alga can be found in shallow waters that are exposed to direct sunlight. However, given that our

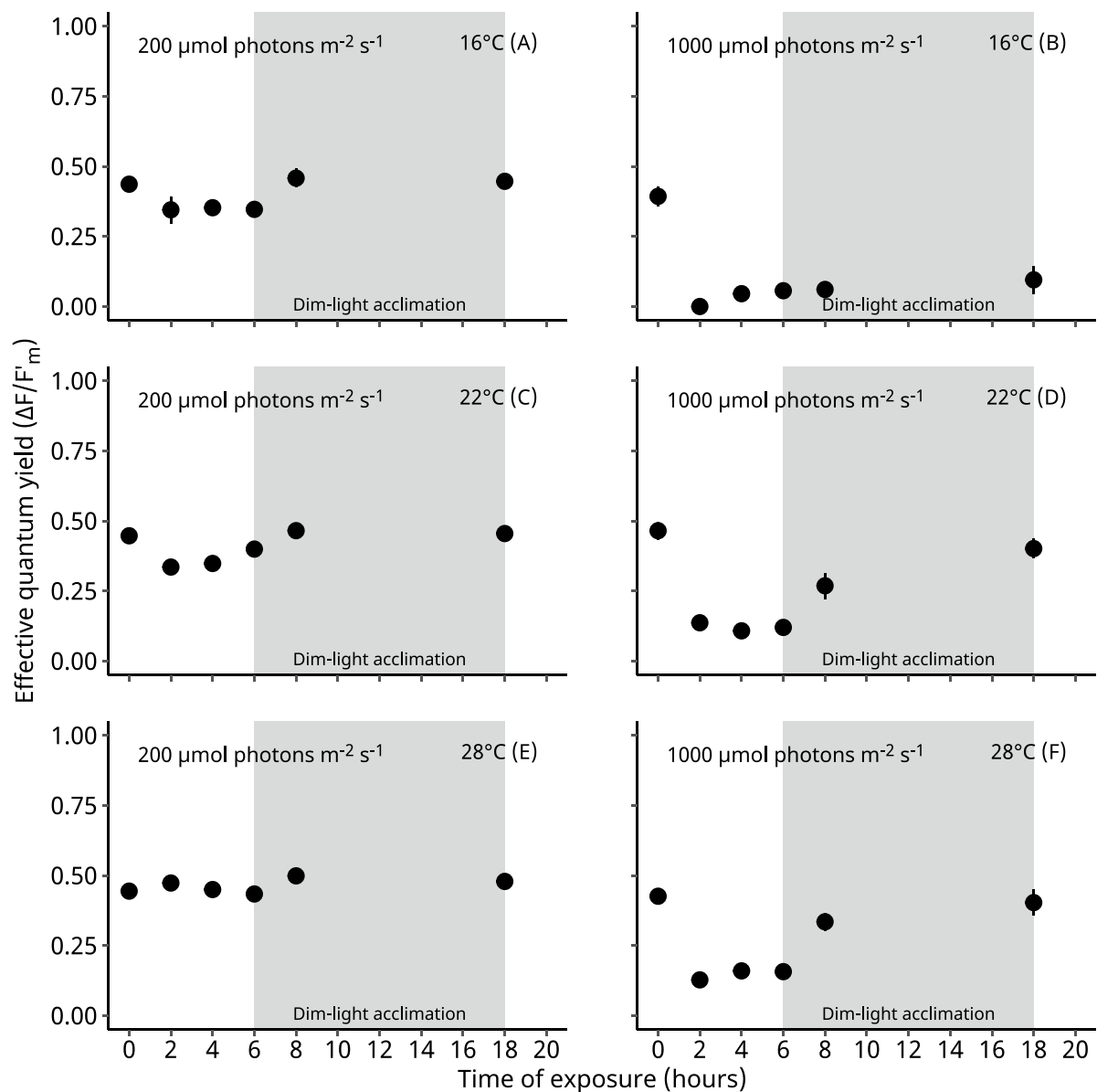


Fig. 8 Hourly changes of the effective quantum yield ($\Delta F/F_m$) in a red alga, *Chondria armata* from Kagoshima, Japan, in response to irradiance at 200 (A, C, E) and 1000 (B, D, F) $\mu\text{mol photons m}^{-2} \text{s}^{-1}$ at 16 (A, B), 22 (C, D), and 28°C (E, F). Symbols and bars represent the mean and standard deviation of observations ($n = 10$). Irradiance

and temperature exposures were conducted for 6 hours. Subsequently, the explants were acclimated for 12 hours under dim light (20 $\mu\text{mol photons m}^{-2} \text{s}^{-1}$). Measurements at 8 hours were conducted to confirm recovery potential at the 2-hour dim-light acclimation level

study site is located near the northern distributional limit, the combination of winter low temperatures and strong sunlight might cause to be significant stress like chilling-light stress. Understanding that the winter environment is close to its threshold level might be important for the conservation of this algal population. Second, as this algae could be found throughout a year in our phenological study, this alga can be regarded to be perennial species that can survive in winter. As for its management for sustainable resources, appropriate collection

procedures (i.e., remaining basal portion for regeneration) seems to be essential.

The distinctive biosynthesis of DA in this alga was recently elucidated along with a unique evolutionary hypothesis (Steele et al. 2022). While the temporal pattern of DA production in this alga remains incompletely understood, it has been reported that the concentration of DA is notably high in winter (January; Noguchi and Arakawa 1996; Park et al. 1999). Should this hold true, the synthesis of DA

in this alga could potentially be linked to its characteristic seasonality, as revealed in the present study. Furthermore, DA concentration of this alga is reported to be enhanced in a high-nutrient environment (N, P, Fe-enhanced medium) under laboratory culture (Jiang et al. 2014), suggesting that this production might also be some kind of response to biotic stress (e.g., cold temperature, high nutrient concentration). However, these mechanisms are still uncertain, including those in the diatom (*Pseudo-nitzschia*). Consequently, we emphasize the necessity of further investigations to enhance our comprehension of the ecology and ecotoxicology associated with this alga.

Supplementary Information The online version contains supplementary material available at <https://doi.org/10.1007/s10811-024-03250-w>.

Acknowledgements We would like to extend our gratitude to Dr. Yuichi Kotaki and Dr. Mari Yotsu-Yamashita for their valuable insights into the characteristics of domoic acid in *C. armata*. All authors have provided consent for the publication of this article.

Authors contributions Terada designed the entire study, conducted it, and prepared the manuscript. Yoshizato and Murakami conducted both the field survey and the laboratory experiments. Nishihara designed the statistical analysis, conducted it, and prepared the figures. All authors participated in the review of the manuscript.

Funding Open access funding provided by Kagoshima University. This study received partial support from the Japan Society for the Promotion of Science (JSPS) through the Grant-in-Aid for Scientific Research (#25340012, #20H03076, 22K05805).

Data availability Datasets generated in the present study are available from the corresponding author upon reasonable request.

Declarations

Competing interests The authors declare no competing interests.

Open Access This article is licensed under a Creative Commons Attribution 4.0 International License, which permits use, sharing, adaptation, distribution and reproduction in any medium or format, as long as you give appropriate credit to the original author(s) and the source, provide a link to the Creative Commons licence, and indicate if changes were made. The images or other third party material in this article are included in the article's Creative Commons licence, unless indicated otherwise in a credit line to the material. If material is not included in the article's Creative Commons licence and your intended use is not permitted by statutory regulation or exceeds the permitted use, you will need to obtain permission directly from the copyright holder. To view a copy of this licence, visit <http://creativecommons.org/licenses/by/4.0/>.

References

Alexandrov GA, Yamagata Y (2007) A peaked function for modeling temperature dependence of plant productivity. *Ecol Model* 200:189–192

Al-Fadhli A, Wahidulla S, D'Souza L (2006) Glycolipids from the red alga *Chondria armata* (Kütz.) Okamura. *Glycobiology* 16:902–915

Allakhverdiev SI, Murata N (2004) Environmental stress inhibits the synthesis de novo of proteins involved in the photodamage-repair cycle of photosystem II in *Synechocystis* sp. PCC 6803. *Biochim Biophys Acta* 1657:23–32

Allakhverdiev SI, Kreslavski VD, Klimov VV, Los DA, Carpentier R, Mohanty P (2008) Heat stress: an overview of molecular responses in photosynthesis. *Photosynthesis Res* 98:541–550

Bellasio C, Burgess SJ, Griffiths H, Hibberd JM (2014) A high throughput gas exchange screen for determining rates of photorespiration or regulation of C4 activity. *J Exp Bot* 65:3769–3779

Borlongan IA, Maeno Y, Kozono J, Endo H, Shimada S, Nishihara GN, Terada R (2019) Photosynthetic performance of *Saccharina angustata* (Laminariales, Phaeophyceae) at the southern boundary of distribution in Japan. *Phycologia* 58:300–309

Borlongan IA, Arita R, Nishihara GN, Terada R (2020) The effects of temperature and irradiance on the photosynthesis of two heteromorphic life history stages of *Saccharina japonica* (Laminariales) from Japan. *J Appl Phycol* 32:4175–4187

Borlongan IA, Suzuki S, Nishihara GN, Kozono J, Terada R (2020) Effects of light quality and temperature on the photosynthesis and pigment content of a subtidal edible red alga *Meristotheca papulosa* (Solieriaceae, Gigartinales) from Japan. *J Appl Phycol* 32:1329–1340

Brassart PL, Thomas OP, Courdavault C, Papon N (2022) Towards a better understanding of toxin biosynthesis in seaweeds. *ChemBioChem* 23:e2022002

Brunson JK, McKinnie SMK, Chekan JR, McCrow JP, Miles ZD, Bertrand EM, Bielinski VA, Luhavaya H, Oborník M, Smith GJ, Hutchins DA, Allen AE, Moore BS (2018) Biosynthesis of the neurotoxin domoic acid in a bloom-forming diatom. *Science* 361:1356–1358

Bürkner PC (2018) Advanced Bayesian multilevel modeling with the R package brms. *R J* 10:395–411

Ciavatta ML, Wahidulla S, D'Souza L, Scognamiglio G, Cimino G (2001) New bromotriterpene polyethers from the Indian alga *Chondria armata*. *Tetrahedron* 57:617–623

Daigo K (1959) Studies on the constituents of *Chondria armata*. I: Detection of the anthelmintical constituents. *Yakugaku Zasshi* 79:350–353 (in Japanese with English abstract)

Fujimoto M, Nitta K, Nishihara GN, Terada R (2014) Phenology, irradiance and temperature characteristics of a freshwater red alga, *Nemalionopsis tortuosa* (Thoreales), from Kagoshima, southern Japan. *Phycol Res* 62:77–85

Govenkar MB, Wahidulla S (2000) Constituents of *Chondria armata*. *Phytochemistry* 54:979–981

Henley WJ (1993) Measurement and interpretation of photosynthetic light-response curves in algae in the context of photo inhibition and diel changes. *J Phycol* 29:729–739

Huang SF (2003) Seaweeds of northeastern Taiwan, 2nd edn. National Taiwan Museum, Taipei (in Chinese)

Huisman JM (2019) Marine plants of Australia, Revised. UWA Publishing, Crawley

Ito T, Borlongan IA, Nishihara GN, Endo H, Terada R (2021) The effects of irradiance, temperature, and desiccation on the photosynthesis of a brown alga, *Sargassum muticum* (Fucales), from a native distributional range in Japan. *J Appl Phycol* 33:1777–1791

Ito T, Yoshioka T, Shimabukuro H, Nishihara GN, Endo H, Terada R (2023) The effect of temperature, light-spectrum, desiccation, and salinity gradients on the photosynthetic performance of a subtidal brown alga, *Sargassum macrocarpum* from Japan. *Phycol Res* 71:25–36

Jassby AD, Platt T (1976) Mathematical formulation of the relationship between photosynthesis and light for phytoplankton. *Limnol Oceanogr* 21:540–547

- Jiang S, Kuwano K, Ishikawa N, Yano M, Takahashi T, Arakawa O (2014) Production of domoic acid by laboratory culture of the red alga *Chondria armata*. *Toxicon* 92:1–5
- Kurahori T, Shimabukuro H, Terada R (2022) Phenology and environmental characteristics of two species of *Sargassum* (Fucales), *S. hemiphyllum* and *S. glaucescens* from Kagoshima Bay, Japan. *Nippon Suisan Gakkaishi* 88:12–19 (in Japanese with English abstract)
- Maeda M, Kodama T, Tanaka T, Yoshizumi H, Takemoto T, Nomoto K, Fujita T (1986) Structure of isodomoic acids A, B and C, novel insecticidal amino acids from the red alga *Chondria armata*. *Chem Pharm Bull* 34:4892–4895
- Maeda M, Kodama T, Tanaka T, Yoshizumi H, Takemoto T, Nomoto K, Fujita T (1987) Structures of domoic acid A and B, novel amino acids from the red alga, *Chondria armata*. *Tetrahedron Lett* 28:633–636
- Maeno Y, Kotaki Y, Terada R, Cho Y, Konoki K, Yotsu-Yamashita Y (2018) Six domoic acid related compounds from the red alga, *Chondria armata*, and domoic acid biosynthesis by the diatom, *Pseudo-nitzschia multiseriata*. *Sci Rep* 8:356
- Mori S, Sugahara K, Maeda M, Nomoto K, Iwashita T, Yamagaki T (2016) Insecticidal activity guided isolation of palytoxin from a red alga, *Chondria armata*. *Tetrahedron Lett* 57:3612–3617
- Mori S, Sugahara K, Maeda M, Shimamoto K, Iwashita T, Yamagaki T (2018) A truncated palytoxin analogue, palytoxin carboxylic acid, isolated as an insecticidal compound from the red alga, *Chondria armata*. *Tetrahedron Lett* 59:4420–4425
- Nishihara GN, Mori Y, Terada R, Noro T (2004) Habitat characteristics and seasonal changes of *Laurencia brongniartii* (Ceramiales, Rhodophyta) in Kagoshima, Southern Japan. *Phycol Res* 52:30–37
- Noguchi T, Arakawa O (1996) Distribution of domoic acid in seaweeds occurring in Kagoshima, southern Japan. In: Singh BR, Tu AT (eds) *Natural toxins 2, Structure, mechanism of action, and detection*. Plenum Press, New York, pp 521–526
- Okamura K (1907) *Icons of Japanese algae*, 1st edn. Kazama Shobo, Tokyo, pp 69–71 pl. 16, figs 9–19
- Okamura K (1936) *Nippon Kaiso Shi*. Uchida-Rokakuho, Tokyo (in Japanese)
- Ospina R, Ferrari SLP (2012) A general class of zero-or-one inflated beta regression models. *Comput Stat Data Anal* 56:1609–1623
- Park HJ, Takatani T, Noguchi T (1999) Screening test of domoic acid in algae shellfishes around Kagoshima where “Hanayanagi” *Chondria armata* inhabits. *Mem Fac Fish Nagasaki Univ* 80:79–81 (in Japanese with English abstract)
- Payri CE (2006) Revised checklist of marine algae (Chlorophyta, Rhodophyta and Ochrophyta) and seagrasses (Marine Angiosperma) of New Caledonia. In: Payri CE, Richer de Forges B (eds) *Compendium of marine species from New Caledonia. Documents Scientifiques et Techniques. II7*, Centre IRD de Nouméa, New Caledonia, pp. 93–110
- Platt T, Gallegos CL, Harrison WG (1980) Photoinhibition of photosynthesis in natural assemblages of marine phytoplankton. *J Mar Res* 38:687–701
- R Development Core Team (2023) R: A language and environment for statistical computing. R Foundation for Statistical Computing, Vienna <http://www.R-project.org> (accessed on 10 August 2023)
- Roleda MY (2009) Photosynthetic response of Arctic kelp zoospores exposed to radiation and thermal stress. *Photochem Photobiol Sci* 9:1302–1312
- Serisawa Y, Taino S, Ohno M, Aruga Y (1998) Succession of seaweeds on experimental plates immersed during different seasons in Tosa Bay, Japan. *Bot Mar* 41:321–328
- Shimabukuro H, Higuchi F, Terada R, Noro T (2007a) Seasonal changes of two *Sargassum* species: *S. yamamotoi* and *S. kushimotoense* (Fucales, Phaeophyceae) at Shibushi Bay, Kagoshima, Japan. *Nippon Suisan Gakkaishi* 73:244–249 (in Japanese with English abstract)
- Shimabukuro H, Terada R, Sotobayashi J, Nishihara GN, Noro T (2007b) Phenology of *Sargassum duplicatum* (Fucales, Phaeophyceae) from the southern coast of Satsuma Peninsula, Kagoshima, Japan. *Nippon Suisan Gakkaishi* 73:454–460 (in Japanese with English abstract)
- Shindo A, Borlongan IA, Nishihara GN, Terada R (2022) Interactive effects of temperature and irradiance including spectral light quality on the photosynthesis of a brown alga *Saccharina japonica* (Laminariales) from Hokkaido, Japan. *Algal Res* 66:102777
- Shimura I, Tanaka T (2008) Useful seaweeds in Kagoshima Prefecture III. Red algae. *Jpn J Phycol* 56:123–128 (in Japanese)
- Silva PC, Basson PW, Moe RL (1996) *Catalogue of the benthic marine algae of the Indian Ocean*. University of California Publications in Botany. Berkeley: University of California Press, p 79
- Stan Development Team (2024) RStan: the R interface to Stan. Version 2.26.24. <http://mc-stan.org>. Accessed on 20 April 2024
- Steele TS, Brunson JK, Maeno Y, Terada R, Allen AE, Yotsu-Yamashita M, Chekan JR, Moore BS (2022) Domoic acid biosynthesis in the red alga *Chondria armata* suggests a complex evolutionary history for toxin production. *Proc Natl Acad Sci USA* 119:e2117407119
- Takahashi S, Murata N (2008) How do environmental stresses accelerate photoinhibition? *Trends Plant Sci* 13:178–182
- Takemoto T, Daigo K (1958) Constituents of *Chondria armata*. *Chem Pharm Bull* 6:578–580
- Tanaka T (1956) Marine algae from the Amami islands and their resources. *Mem South Indus Inst Kagoshima Univ* 1:13–22 (in Japanese)
- Tani M, Masuda M (2003) A taxonomic study of two minute species of *Chondria* (Ceramiales, Rhodophyta) from the north-western Pacific, with the description of *Chondria econstricta* sp. nov. *Phycologia* 42:220–231
- Tcherkez G, Bligny R, Gout E, Mahé A, Hodges M, Cornic G (2008) Respiratory metabolism of illuminated leaves depends on CO₂ and O₂ conditions. *Proc Natl Acad Sci USA* 105:797–802
- Terada R, Matsumoto K, Borlongan IA, Watanabe Y, Nishihara GN, Endo H, Shimada S (2018) The combined effects of PAR and temperature including the chilling-light stress on the photosynthesis of a temperate brown alga, *Sargassum patens* (Fucales), based on field and laboratory measurements. *J Appl Phycol* 30:1893–1904
- Terada R, Nakashima Y, Borlongan IA, Shimabukuro H, Kozono J, Endo H, Shimada S, Nishihara GN (2020) Photosynthetic activity including the thermal- and chilling-light sensitivities of a temperate Japanese brown alga *Sargassum macrocarpum*. *Phycol Res* 68:70–79
- Terada R, Abe M, Abe T, Aoki M, Dazai A, Endo H, Kamiya M, Kawai H, Kurashima A, Motomura T, Murase N, Sakanishi S, Shimabukuro H, Tanaka J, Yoshida G, Aoki M (2021) Japan’s nationwide long-term monitoring survey of seaweed communities known as the ‘Monitoring Sites 1000’: Ten-year overview and future perspectives. *Phycol Res* 69:12–30
- Terada R, Nishihara GN, Arimura K, Watanabe Y, Mine T, Morikawa T (2021) Photosynthetic response of a cultivated red alga, *Neopyropia yezoensis* f. *narawaensis* (= *Pyropia yezoensis* f. *narawaensis*; Bangiales, Rhodophyta) to dehydration stress differs with between two heteromorphic life-history stages. *Algal Res* 55:102262
- Terada R, Takaesu M, Borlongan IA, Nishihara GN (2021) The photosynthetic performance of a cultivated Japanese green alga *Caulerpa lentillifera* in response to three different stressors, temperature, irradiance, and desiccation. *J Appl Phycol* 33:2547–2559
- Terada R, Nakamura R, Iwanaga T, Nakahara K, Nishihara GN (2023) The real-time measurements of PSII photochemical efficiency in the microscopic sporophyte of *Pyropia yezoensis*

- f. *narawaensis* (Bangiaceae) reveals the low capacity of desiccation tolerance that drops within a few minutes of dehydration. *Algal Res* 75:103283
- Terada R, Shindo A, Moriyama H, Shimboku N, Nishihara GN (2023) The response of photosynthesis to temperature and irradiance in a green alga, *Ryugophycus kuaweuweu* (Ulvales) reveals adaptation to a subtidal environment in the northern Ryukyu Islands. *Algal Res* 74:103189
- Wang WL, Chiang YM (1994) Potential economic seaweeds of Hengchun Peninsula, Taiwan. *Econ Bot* 48:182–189
- Webb WL, Newton M, Starr D (1974) Carbon dioxide exchange of *Alnus rubra*: a mathematical model. *Oecologia* 17:281–291
- Wright JLC, Boyd RK, de Freitas ASW, Falk M, Foxall RA, Jamieson WD, Laycock MV, McCulloch AW, McInnes AG, Odense P, Pathak VP, Quilliam MA, Ragan MA, Sim PG, Thibault P, Walter JA, Gilgan M, Richard DJA, Dewar D (1989) Identification of domoic acid, a neuroexcitatory amino acid, in toxic mussels from eastern Prince Edward Island. *Can J Chem* 67:481–490
- Yamagishi Y, Miwa Y (2008) Marine algal flora of Fukuyama and Innoshima Island, central region of Seto Inland Sea. *Ann Rep Fac Life Sci Biotechnol Fukuyama Univ* 7:21–33 (in Japanese)
- Yoshida T (1998) Marine algae of Japan. Uchida-Phokakuho, Tokyo (in Japanese)
- Zaman L, Arakawa O, Shimosu A, Onoue Y, Nishino S, Shida Y, Noguchi T (1997) Two new isomers of domoic acid from a red alga, *Chondria armata*. *Toxicon* 35:205–212

Publisher's Note Springer Nature remains neutral with regard to jurisdictional claims in published maps and institutional affiliations.